Photovoltaic Power Prediction from Medium-Range Weather Forecasts: a Real Case Study

Alessandro Ciocia, Gianfranco Chicco, Alessandro Gasperoni, Gabriele Malgaroli, Filippo Spertino
[1]Dipartimento Energia "Galileo Ferraris", Politecnico di Torino, Torino, Italy
{alessandro.ciocia, gianfranco.chicco, gabriele.malgaroli, filippo.spertino}@polito.it,
alessandro.gasperoni@studenti.polito.it

Abstract— The aim of this work is to utilize weather forecasts with a lead time from 6 h to 30 h as input data of a photovoltaic (PV) model to predict the AC power production. In order to always use the last forecasts, the inputs are updated every time there are new data, e.g., every 6 h. The ability of the model is tested on a residential PV plant for which global irradiance and electrical power are measured. The typical indicators of forecast accuracy in the PV applications are used: mean bias error and mean absolute error for both irradiance and power. However, they are normalized with respect to the standard irradiance and the PV rated power. Their values are generally adequate in clear sky and overcast conditions, remaining around the 10% limit.

Keywords—Photovoltaic generation, weather forecast, prediction, PV system, measurements.

I. Introduction

Regarding the contribution of photovoltaic (PV) energy towards energy transition and decarbonization, in Italy the potential is noticeable with respect to many other European countries. Renewable sources have also disadvantages, the main one being undoubtedly the intermittency of the resource during the day (besides the obvious day-night cycle) with the consequent difficulty to predict the PV production profile in case of clouds passage on the skye [1].

A. Weather Forecast Data Classification

The main way in which predictions for PV generation can be classified is according to time horizon of weather data forecasts. Very short-term forecasts (intra-day) have a time base of 5÷60 min, and the applications are adjustments/dispatching, market clearing and contingency analysis. Short range (or short-term, from 1 h to 6 h in advance) forecasts are used for resource scheduling and congestion management. Finally, medium-range forecasts have a time base of days, with applications to reserve scheduling, congestion management and energy trading [2].

B. Model Typologies for PV Predictions

An important distinction among prediction models is made according to the type of model used. In particular, the models can be physical, statistical or hybrid. Physical models use exogenous data (temperature, wind speed and direction, irradiance, cloud cover, …), which may come from local measurements, satellites images, numerical weather prediction (NWP), values from other meteorological databases and neighbouring plants. Then, a PV performance model with its analytical equations is applied to generate PV power predictions. For these reasons, this approach is also referred as "white box" method [2, 3]. On the other side, statistical models rely primarily on endogenous past data to train models, with little or no reliance upon theoretical PV models. The statistical models are based on data to extract patterns from past records to predict future PV plant behaviour. The power output can be directly calculated without the need for meteorological predictions, with the sometimes called "direct method." Unlike physical models, statistical techniques result in a "black box" model. Therefore, high-quality historical data are necessary for reaching precise predictions. In contrast to the parametric approach, a large historical dataset is usually required, assuming that the PV plant has already been operational for a while. This approach has the advantage of correcting systematic errors related to input measurement. Selecting an appropriate training dataset is critical for achieving high accuracy in the resulting model. Finally, to increase the accuracy of the forecasts, hybrid models are used. They consist of the combination of the above-described methods. The hybrid approach can be divided into two subcategories: two or more statistical techniques (hybrid-statistical) can be combined, or a statistical technique is incorporated into a PV performance model (hybrid-physical) [4].

Another classification can be made on the spatial basis. Forecasts can be made for a single PV system or for an ensemble of them. Normally, grid operators prefer regional forecasts since they are more useful to keep the balance between demand and supply in the electric system. Variability in power output is reduced when an ensemble of plants is considered, since the forecast error increases with the variability of the signal to forecast.

For example, the approach used in [4] to predict regional PV power output is based on irradiance forecasts provided by the European Centre for Medium-Range Weather Forecasts (ECMWF) [5]. They evaluated the forecast error for the single site, an ensemble covering the area of 220x220 km and the whole area of Germany. A temporal averaging procedure was then applied. They tried different approaches; the best results were obtained combining the forecast data with a clear sky model, then correcting the systematic deviations with a bias correction. The evaluation of the PV power prediction scheme resulted in a root mean square error (*RMSE*) of 0.11 kW/kW$_{peak}$ for single systems. For the ensemble power prediction for an area of 220 km x 220 km, an *RMSE* of 0.06 kW/kW$_{peak}$ was found, and for a larger ensemble covering the area of Germany the *RMSE* was 0.05 kW/kW$_{peak}$ [4].

In the papers [6] and [7], the prediction of alternating current (AC) power for PV plants (with rated power of 1 MW) in Southern Italy (latitude of 40° North) was performed thanks to weather forecasts based on Meteosat images [8] from 1 to 3 days ahead. The weather forecasts were compared with the measurements (1 min profiles) provided by two meteorological stations in the neighbourhood of the PV systems. The papers confirmed that the 1-day ahead forecast of solar irradiance was the best, providing normalized root mean square errors lower than 120 W/m^2, and that the improvement with respect to 2 or 3 days ahead forecasts was more relevant in days with variable weather rather than clear sky ones. A PV conversion model permits to evaluate the AC production: the errors of predicted AC power, exceeded by 5% of the number of quarters of hour in one year, were lower than ±13% of the rated PV power for the two systems analysed.

In this paper, the model used is deterministic, i.e., it uses as inputs all the meteorological data of the analysed location and the physical parameters of the PV system. The output is an hourly power profile that is compared with the measured electrical power.

This paper is organized as follows. Section II contains the description of the physical model used to calculate the photovoltaic production profiles. In Section III, the methodology to obtain the profiles of measured irradiance and electrical load profiles, as well as the forecast meteorological data, are described. Section IV shows the results on two time scales – on a daily basis to compare the predicted and actual PV profiles; on the whole simulation period to estimate the global performance of the model. Finally, the conclusions summarise the main findings of the paper.

II. Modelling of PV Power Generation

The irradiance G and air temperature T_a profiles (mean hourly data) are the inputs used in this paper for calculating the output power of a PV generator. In particular, the active power production at the AC side is proportional to the product of the power at the direct current (DC) side by the inverter efficiency η_{conv}. The DC/AC inverter losses can be modelled as a quadratic function of the output power [9], which considers the losses in the DC/AC conversion and transformation, including the consumption of the auxiliary circuits (control, measurement, and cooling).

$$P_{AC} = P_{DC} \cdot \eta_{CONV} = (P_{STC} \cdot \eta_G \cdot C_T \cdot \eta_{mix}) \cdot \eta_{CONV} \qquad (1)$$

Regarding the calculation of the DC power output of the PV systems P_{DC} (kW), it is proportional to the product of:

- The nominal power of the plant P_{STC} (power calculated at Standard Test Conditions, STC [9]).

- The parameter $\eta_G = (G-G_0)/G_{STC}$ is the ratio of the global irradiance G (reduced by a low threshold of irradiance G_0 [10], and the standard irradiance of 1000 W/m^2.
- The thermal coefficient $C_T = 1+\gamma_T \cdot (T_c$-25°C) depends on the thermal coefficient of power ($\gamma_T \approx$-0.5%/°C) and on the temperature T_c of the PV modules, calculated as a function of G and T_a, according to the NOCT formula [11, 12].
- The parameter η_{mix}, which includes different sources of losses, e.g., dirt, reflection, mismatch, joule losses in cables, and MPPT accuracy [13].

Irradiance data are available on the horizontal plane; therefore, they are calculated for the plane of PV array by means of the Equation (2) from the ASHRAE model. This model refers to clear sky conditions and calculates the global irradiance components as a function of the geographical coordinates and the time of the year [14]:

$$G = \frac{BHI}{\cos(\theta_z)} \cdot \cos(\theta) + DHI \cdot F_{CS} + \rho \cdot GHI \cdot (1 - F_{CS}) \quad (2)$$

In (2), *BHI* is the direct (or beam) horizontal irradiance, i.e., the irradiance component reaching the ground on a horizontal plane without being reflected nor absorbed by atmosphere. To calculate the contribution of direct component, the solar zenith angle θ_z is used; it is the angle between the Sun's rays and the Zenith axis (perpendicular to the ground). On the other hand, θ is the sun rays' angle of incidence, namely, the angle between the perpendicular to the plane of array and the Earth-Sun line. In the first term of G, the ratio of the two cosine functions is normally higher than unity, making the global irradiance on the tile angle higher than the horizontal irradiance. The second component is the diffuse horizontal irradiance (*DHI*), i.e., the component reaching the ground on a horizontal plane after being reflected by the atmosphere. In this case, the parameter used to calculate it is the Earth-sky view factor F_{cs}. The last contribution is the irradiance reflected by the surrounding ground (usually with negligible contribution). It depends on the albedo coefficient ρ.

III. Irradiance vs. Power Measurements and Processing of Weather Data Forecast

In the present work, measurements are performed to obtain irradiance profiles and electrical power production data in a case-study site. For the same site, weather data forecasts are downloaded, and applying the PV model, AC power is predicted. All these profiles are used for two purposes: first, to calculate the deviation between measured and forecast irradiance. Secondly, to calculate the deviation between the PV model output and the measured AC production.

A. Irradiance and AC Power Measurement

The case study presented in this work is related to a PV system installed in 2015 with nominal power P_{STC}=4.25 kW and polycrystalline silicon modules. The plant is installed 20 km far from Turin, in Northern Italy. It is equipped with irradiance sensors and monitored by an AC measuring system. The solar irradiance is measured by using a calibrated monocrystalline PV cell. The Spektron 210 cell provides a voltage proportional to the intensity of the solar irradiance, approximatively 75 mV at 1000 W/m², with a sensor accuracy of ±5% (annual mean). The PV cell is connected to a data acquisition system ICP DAS I-7017, with 16-bit resolution and sampling rate up to 10 Hz. Then, data are accessed by a PC with a monitoring software. It allows to remotely control the DAS and store data in a database. The AC power output is measured by an HT Solar300. It is a multifunction device for verification of single-phase and three-phase PV system efficiency and power quality analysis. The accuracy is 5% for AC power, while the timestep of data measurements is selected equal to 1 minute. The measurements refer to the period between December 2021 and February 2022.

B. Weather Data Forecast Acquisition

Meteorological variables that influence PV energy production (solar radiation, wind speed, temperature…) at the Earth's surface can be accessed in three forms: measurements from ground-based instruments (e.g., irradiance sensors, anemometers, or thermometers), remote-sensing retrievals (e.g., satellite image processing), and output of dynamical weather models.

These three forms of information, though describing the same quantities, should be regarded as complementary, rather than substitutive [15]. In the present work, forecast weather data profiles are calculated by the ECMWF. They perform combination of the above-mentioned techniques and further data elaboration.

NWP forecasts only stay online for a few days, therefore forecast data are automatically downloaded multiple times per day with an Application Programming Interface (API) made by the authors in MATLAB® and stored in a server, to avoid the loss of the forecasts.

To compute predictions of PV generation, the main weather profiles are irradiance components (for the correction to the array plane described in Section II) and air temperature. Additionally, the other parameters useful to calculate the PV production using other models are the wind speed [m/s], and the cloud covers. Cloud covers are levels of coverage of the sky by the presence of clouds at different altitudes [15].

The spatial resolution can be up to 0.0012° (~90 m at European latitudes). The temporal resolution is 1 h, and the updates of the forecasts occur 4 times per day (at 00:00 AM, 06:00 AM, 12:00 AM, and 06:00 PM), because the time required to perform all the forecast calculations is 6 h.

C. Weather Forecast Data Organization

As written before, forecasts are updated every 6 h. For each query, the downloaded forecast data consist of an hourly data profile up to 72 h in the future. In this work, the first 30 values, i.e., one day plus six hours in advance, are analysed. The lead time of a forecast is the time difference (in hours) between the time of the query and the moment in which the NWP models started the simulation. For example, at 00:00 on 15th Feb, the forecasts are available and immediately downloaded. The data vector contains 30 values, in which the first one is the weather data at 00:00 on 15th Feb and the last values refers to 06:00 AM on 16th Feb. Thus, the first value is that one corresponding to the moment of the download, but having a simulation time of 6 h to calculate weather forecasts, all this profile came from calculations started at 18:00 on 14th Feb. The profile with 30 values in advance is disassembled to create 5 different profiles with lead time of 6h, 12h ,18h, 24h and 30h. For the sake of clarity, the example of the creation of the forecast profiles for the 15th Feb is shown in Fig.1 with only the most and the less recent forecast.

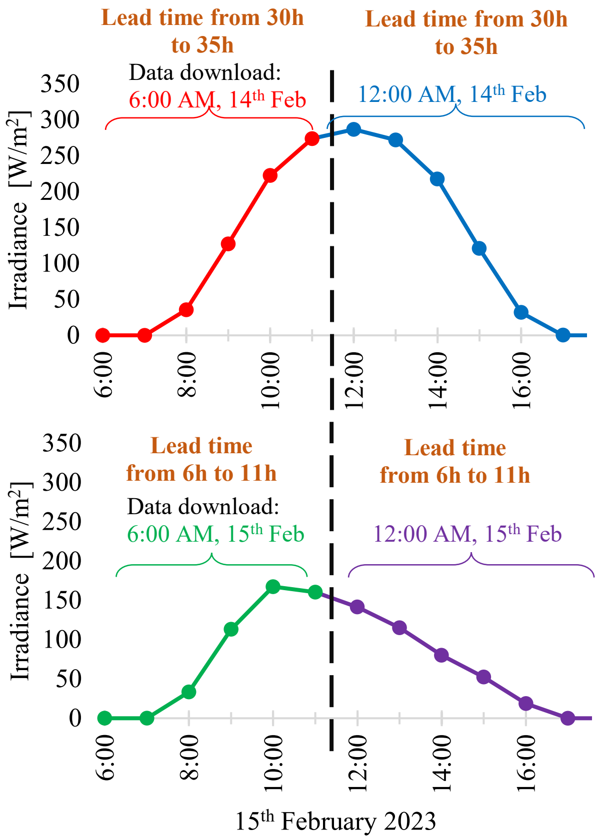

Fig. 1. Creation of forecast profiles: example referring to 15th Feb.

To create the profile with always the last available forecast (lead time = +6h, bottom of Fig.1), data are downloaded at 6:00 AM on 15th Feb for the morning, and at 12:00 AM on 15th Feb for the afternoon. In the same way, to create the profile for the 15th Feb with always a lead time = +30h (top of Fig.1) data are downloaded at 6:00 AM on 14th Feb for the morning, and at 12:00 AM on 14th Feb for the afternoon. The same procedure is repeated for lead times of 12h, 18h and 24h. The software automatically performs this operation every 6h updating the five profiles.

Regarding the lead time for each of the five profiles, it is not constant. Referring to the previous example, the data corresponding to 02:00 AM on 15th Feb is the result of the elaboration started at 18:00 on 14th Feb, thus the lead time is 8 h. In the same way the data corresponding to 05:00 AM on 15th Feb is the result of the elaboration started at 18:00 on 14th Feb, thus the lead time is 11 h. Table I summarises the lead time variation. The second column includes data downloaded 6 h in advance, where the lead time can be between 6 and 11 h. As general rule, the lead time is equal to query time plus a maximum of five hours.

TABLE I. FORECAST LEAD TIME FOR THE FIVE TIME-HORIZON PROFILES.

		Query Time				
Actual time		**6 h**	**12 h**	**18 h**	**24 h**	**30 h**
06:00	Lead time (h)	+6	+12	+18	+24	+30
07:00		+7	+13	+19	+25	+31
08:00		+8	+14	+20	+26	+32
09:00		+9	+15	+21	+27	+33
10:00		+10	+16	+22	+28	+34
11:00		+11	+17	+23	+29	+35
12:00		+6	+12	+18	+24	+30
13:00		+7	+13	+19	+25	+31
14:00		+8	+14	+20	+26	+32
15:00		+9	+15	+21	+27	+33
16:00		+10	+16	+22	+28	+34
17:00		+11	+17	+23	+29	+35

IV. ANALYSIS OF WEATHER DATA FORECASTS AND PV PRODUCTION PREDICTIONS

A. Comparison of Irradiance Profiles

Fig. 2 shows the example of a day which was at first forecasted as a sunny day and it turned out to be very cloudy (or overcast). It displays the five forecast profiles (GHI_{fore}) described in section II (in terms of hourly average power) and the actual measurements GHI_{meas} (with 1-min time step). This is a day which perfectly represents the benefits of updating the forecast more times per day, because each update corresponds to a forecast value closer to the actual one. In the literature, a parameter commonly used to compare the profiles is the *RMSE*. Nevertheless, as indicated in [7], the mean bias of the error (*MBE*) works better for the accuracy evaluation of forecasts, because the AC power generated from PV plants is not a square function of irradiance and *MBE* represents the systematic part of the error. Considering *N* values:

$$MBE = \frac{1}{N}\sum_{i=1}^{N}\left(GHI_{fore} - GHI_{meas}\right)_i \qquad (3)$$

Another parameter is the mean absolute error (*MAE*), which is more sensitive to high-value errors, useful in those applications insensitive to minor error. It is calculated as:

$$MAE = \frac{1}{N}\sum_{i=1}^{N}\left|\left(GHI_{fore} - GHI_{meas}\right)_i\right| \qquad (4)$$

According to [8], the *MBE* index is reported per unit with respect to G_{STC}=1 kW/m^2 in case of irradiance profiles, while *MBE* is divided by the nominal power of the PV generator P_{STC}. In case of power profiles, the equations are the same, but instead of irradiances *GHI*, power values are compared. The parameters for the profiles in Fig. 2 are shown in Table II, in which GHI_{avg} is the average measured irradiance.

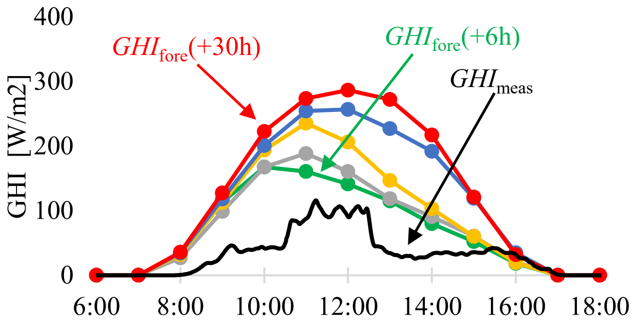

Fig. 2. Improvement in GHI forecast for a cloudy day (15th Feb 2022).

TABLE II. COMPARISON BETWEEN FORECAST AND MEASURED IRRADIANCE PROFILES – EXAMPLE OF A CLOUDY DAY

	GHI_{avg} [kW/m^2]	MBE/G_{STC} [-]	MAE/G_{STC} [-]
Measured	0.040	-	-
t+6	0.088	0.051	0.052
t+12	0.093	0.057	0.058
t+18	0.111	0.076	0.077
t+24	0.144	0.111	0.111
t+30	0.159	0.128	0.128

The day shown in Fig. 2 is used as an example, because it well represents the average situation for the cloudy days. The differences between *MBE* and *MAE* are negligible, because the predictions almost always overestimate the production. Regarding sunny days, there is no large variation of forecasts, with the result that the profiles are almost overlapped. Thus, for sake of clarity, in Fig. 3 only the most recent and the less recent forecasts are shown.

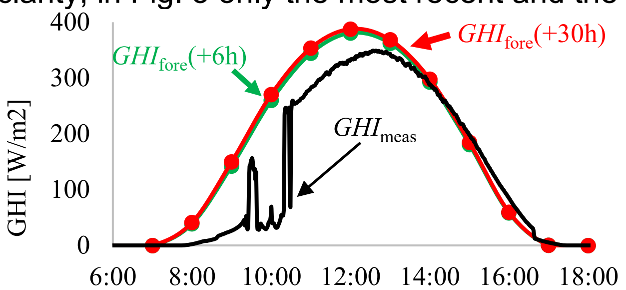

Fig. 3. Progressive improvement in irradiance forecasts for an almost clear-sky day (10th Jan 2022).

TABLE III. COMPARISON BETWEEN FORECAST AND MEASURED IRRADIANCE PROFILES – EXAMPLE OF AN ALMOST CLEAR-SKY DAY

	GHI_{meas} [kWh/m^2]	MBE/G_{STC} [-]	MAE/G_{STC} [-]
Measured	0.165	-	-
t+6	0.203	0.042	0.044
t+12	0.207	0.043	0.045
t+18	0.207	0.044	0.046
t+24	0.208	0.046	0.047
t+30	0.208	0.048	0.049

As shown in Table III, in this day (that well represents all the sunny days in the period under analysis), the indicators are always lower than 5%.

As in the previous case, also *MBE* indicators are always positive, because the predictions overestimate the production.

B. Comparison of PV production profiles

Fig. 4 shows the comparison between the less recent prediction P_{fore}(+30h), the most recent prediction P_{fore}(+6h), and measurements (P_{meas}) of AC production from the PV plant in a cloudy day in February. The AC power predictions are obtained by using the PV model with weather data forecasts as inputs. In the graph, predicted and measured AC profiles are hourly average powers (AC power measurements with 1-min step are averaged to obtain hourly values). In this case, there is a remarkable improvement in the last prediction compared to the initial prediction that led to an important energy overestimation. In fact, MBE/P_{STC} decreases from 12% to 3%, while MAE/P_{STC} decreases from 19% to 11%. Table IV summarizes the comparison of the plotted profiles on a daily basis, where P_{avg} is the average measured power.

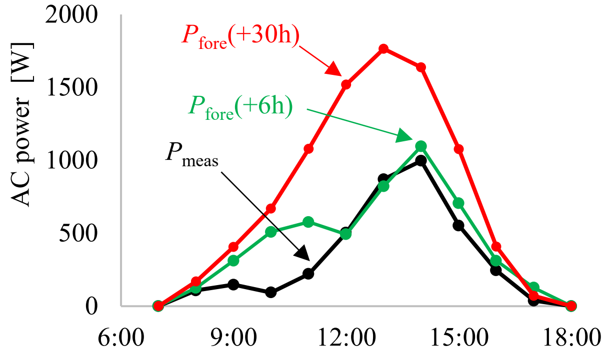

Fig. 4. Progressive improvement in the AC power predictions for a cloudy day (6th Feb 2022).

TABLE IV. Comparison Between Prediction and Measurements of PV Power Production – Example of a Cloudy Day

	P_{avg} [kW]	MBE/P_{STC} [-]	MAE/P_{STC} [-]
Measured	0.343	-	-
t+6	0.460	0.032	0.110
t+30	0.802	0.125	0.192

Fig. 5 shows an example of comparison between actual PV production and predicted profiles in case of a clear sky day. The prediction profiles are accurate also 30 h in advance and the related profile is overlapped with the most recent profile (lead time of +6 h). In both cases, MBE/P_{STC} is negligible and MAE/P_{STC} is less than 3%. Table V summarizes the comparison of the plotted profiles on a daily basis.

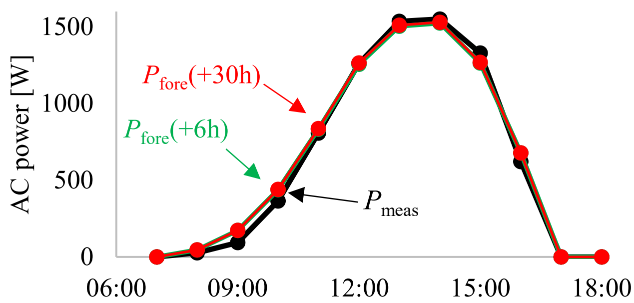

Fig. 5. Example of progressive improvement in AC power predictions for a clear sky day (15th Jan 2022).

TABLE V. Comparison Between Prediction and Measurements of PV Power Production – Example of a Clear-Sky Day

	P_{avg} [kW]	MBE/P_{STC} [-]	MAE/P_{STC} [-]
Measured	0.711	-	-
t+6	0.706	0.003	0.025
t+30	0.705	0.004	0.025

Finally, Table VI presents the *MAE* parameter calculated for the whole three months under analysis (Dec 21 – Feb 22). The first row refers to irradiance, while the second one is related to power profiles. The results are close to a clear sky day, because even though it was winter, rains have been very scarce due to the drought period occurring in the last years in Northern Italy. For this reason, there are negligible differences between t+6 and t+30 profiles.

TABLE VI. COMPARISON BETWEEN PREDICTIONS AND MEASUREMENTS DEC 21 – FEB 22

	t+6	t+12	t+18	t+24	t+30
MAE/G_{STC}	5.2%	4.8%	4.7%	4.8%	4.8%
MAE/P_{STC}	2.8%	2.6%	2.5%	2.5%	2.3%

V. CONCLUSIONS

In this paper, a double comparison of irradiance forecasts vs. irradiance measurements, and power forecasts vs. power measurements, has been presented for a PV system located in Northern Italy. A medium-range forecast with a lead time from 6 h to 30 h, within a maximum duration of 72 h ahead forecast, has been used to provide the most accurate forecasts.

The results are aligned with the analysis in the literature, demonstrating that forecasts of irradiance and predictions of power are adequate in case of both clear sky and cloudy days.

Indeed, in the clear sky days, the typical indicators, both mean bias error and mean absolute error, with respect to G_{STC}, are less than 5%. These parameters do not change from 30 h to 6 h in advance; thus, the less recent forecast is already adequate. On the contrary, in case of cloudy days, the same indicators can increase reaching ≈13% by using a 30 h ahead forecast. However, these indicators can go back to ≈5%, if the 6 h ahead forecast is used.

Then, regarding PV power profiles in the clear sky days, the mean bias error is negligible, and the mean absolute error can be lower than 3%. In a way similar to irradiance forecasts, it has been quantitatively shown how much more recent power predictions can provide better results. In a typical cloudy day, the mean bias error with respect to P_{STC} decreases from 12% to 3%, and the mean absolute error with respect to P_{STC} decreases from 19% to 11%.

In future works, the authors will extend this analysis to a higher numbers of PV plants, with different nominal power and a longer timeframe for the comparison of the profiles. Moreover, the data will be separated and analysed according to the level of cloud coverage. With these results, the authors will optimize the parameters of the PV production model to minimize the energy deviations resulting from the use of the forecasts.

REFERENCES

[1] P.X. Fang, J. Tan, H. Yuan, S. Yin, and J. Wang, "Providing Ancillary Services with Photovoltaic Generation in Multi-Timescale Grid Operation: Preprint," 2021, Accessed: Apr. 30, 2023. [Online]. Available: www.nrel.gov/publications.

[2] J. Antonanzas, N. Osorio, R. Escobar, R. Urraca, F. J. Martinez-de-Pison, and F. Antonanzas-Torres, "Review of photovoltaic power forecasting," *Solar Energy*, vol. 136, pp. 78–111, Oct. 2016.

[3] IEA, "Photovoltaic and Solar Forecasting: State of the Art Report," IEA PVPS T14-01:2013 Forecast PV power Actual PV power Forecast PV power Actual PV power.

[4] M. Schneider, H. G. Beyer, D. Heinemann, G. Karampela, J. Hurka, and E. Lorenz, "Qualified Forecast of Ensemble Power Production by Spatially Dispersed Grid-Connected PV Systems," 23rd European Photovoltaic Solar Energy Conference and Exhibition, 1-5 September 2008, Valencia, Spain, pp. 3285–3291, Nov. 2008.

[5] D. Yang, W. Wang, and T. Hong, "A historical weather forecast dataset from the European Centre for Medium-Range Weather Forecasts (ECMWF) for energy forecasting," *Solar Energy*, vol. 232, pp. 263–274, Jan. 2022.

[6] G. Chicco, V. Cocina, P. Di Leo, and F. Spertino, "Weather forecast-based power predictions and experimental results from photovoltaic systems", 2014 International Symposium on Power Electronics, Electrical Drives, Automation and Motion, SPEEDAM 2014, pp. 342–346, 2014.

[7] G. Chicco, V. Cocina, P. Di Leo, F. Spertino, and A. Massi Pavan, "Error Assessment of Solar Irradiance Forecasts and AC Power from Energy Conversion Model in Grid-Connected Photovoltaic Systems", *Energies*, vol. 9, no. 1, Dec. 2015, doi: 10.3390/EN9010008.

[8] Meteosat, Meteosat On Line animazioni satelliti meteo, previsioni fino a 5 giorni, meteo attuale. https://www.meteosatonline.it/ (accessed Apr. 30, 2023).

[9] A. Ciocia, J. Ahmad, G. Chicco, P. Di Leo, and F. Spertino, “Optimal size of photovoltaic systems with storage for office and residential loads in the Italian net-billing scheme”, Proceedings - 2016 51st International Universities Power Engineering Conference, UPEC 2016, vol. 2017-January, pp. 1–6, Jul. 2016.

[10] A. Ciocia et al., “Self-Consumption and Self-Sufficiency in Photovoltaic Systems: Effect of Grid Limitation and Storage Installation”, *Energies*, vol. 14, art. 1591, vol. 14, no. 6, p. 1591, Mar. 2021.

[11] G. Antonetto et al., “Synergistic freshwater and electricity production using passive membrane distillation and waste heat recovered from camouflaged photovoltaic modules”, *J Clean Prod*, vol. 318, p. 128464, Oct. 2021.

[12] P. Di Leo, F. Spertino, S. Fichera, G. Malgaroli, and A. Ratclif, “Improvement of self-sufficiency for an innovative nearly zero energy building by photovoltaic generators”, 2019 IEEE Milan PowerTech, Jun. 2019.

[13] F. Spertino et al., “A power and energy procedure in operating photovoltaic systems to quantify the losses according to the causes”, *Solar Energy*, vol. 118, pp. 313–326, Aug. 2015.

[14] A.A.M. Omara, A.A.A. Abuelnuor, and I.A.I. Eshag, “Estimation of Solar Radiation of Khartoum City Using ASHRAE Model”, Proceedings of: 2020 International Conference on Computer, Control, Electrical, and Electronics Engineering, ICCCEEE 2020, Feb. 2021.

[15] Meteomatics, *Meteomatics meteorological service*, Available online: https://www.meteomatics.com/en/about-us/ (accessed Apr. 30, 2023).